Saudi Journal of Biological Sciences 27 (2020) 1066–1072

Contents lists available at ScienceDirect

Saudi Journal of Biological Sciences

journal homepage: www.sciencedirect.com

Original article

Application of radiography of computed tomography in non-small cell lung cancer using prognosis model

Yifeng Jin [a], Tao Lu [b,*]

[a] Department of Respiratory, Zhuji Affiliated Hospital of Shaoxing University, Zhuji 311800, China
[b] Department of Radiology, Fujian Cancer Hospital, Fujian Medical University Cancer Hospital, Fuzhou City, Fujiang Province 350014, China

ARTICLE INFO

Article history:
Received 11 October 2019
Revised 25 February 2020
Accepted 26 February 2020
Available online 4 March 2020

Keywords:
Prognostic model
CT radiography
NSCLC
Optimal feature
5-Fold cross-validation

ABSTRACT

Objective: Studying the diagnostic value of CT imaging in non-small cell lung cancer (NSCLC), and establishing a prognosis model combined with clinical characteristics is the objective, so as to provide a reference for the survival prediction of NSCLC patients.
Method: CT scan data of NSCLC 200 patients were taken as the research object. Through image segmentation, the radiology features of CT images were extracted. The reliability and performance of the prognosis model based on the optimal feature number of specific algorithm and the prognosis model based on the global optimal feature number were compared.
Results: 30-RELF-NB (30 optimal features, RELF feature selection algorithm and NB classifier) has the highest accuracy and AUC (area under the subject characteristic curve) in the prognosis model based on the optimal features of specific algorithm. Among the prognosis models based on global optimal features, 25-NB (25 global optimal features, naive Bayes classification algorithm classifier) has the highest accuracy and AUC. Compared with the prediction model based on feature training of specific feature selection algorithm, the overall performance and stability of the prediction model based on global optimal feature are higher.
Conclusion: The prognosis model based on the global optimal feature established in this paper has good reliability and performance, and can be applied to the CT radiology of NSCLC.

1. Introduction

If the growth of lung tissue cells is uncontrolled, it will lead to a malignant lung tumor, like lung cancer (Namkoong et al., 2017). As one of the malignant tumors that pose the greatest threat to people's health and life, its morbidity and mortality are also the fastest growing. If it is not treated, tumor cells will transfer to adjacent tissues as well as other parts of the body (Huang and Soo, 2017). According to histopathology, there are two categories of lung cancer: small cell lung cancer (SCLC) and non-small cell lung cancer (NSCLC) (Casiraghi et al., 2017). NSCLC is lung epithelial cancer except SCLC, accounting for about 80% of all lung cancers. Its high-risk factors include smoking, ionizing radiation, previous chronic lung infection, air pollution, occupational and environmental exposure, and genetics, etc. (Beth Eaby-Sandy, 2017). It includes squamous cell carcinoma, adenocarcinoma, as well as large cell carcinoma. The growth cancer cells is slow and it has a slower metastatic spread (Kato et al., 2018). Therefore, NSCLC patients are usually found in the middle as well as advanced stage. The survival rate is very low, which are 5 years (Namani et al., 2017). The clinical manifestations of patients are relatively complex. According to the severity of the disease, cough, bloody sputum or hemoptysis, chest pain, fever, emaciation and cachexia, or other extrapulmonary symptoms may occur (Hui et al., 2017). NSCLC can be found on chest radiography or tomography, and can be diagnosed by bronchoscopy or CT-guided biopsy (Lin et al., 2017).

Image radiomics can be intuitively understood as quantitative research by transforming visual image information into deep features (Kamaleshwaran et al., 2017). Among them, computed tomography (CT) images refer to the cross-sectional scanning of a specific part of the human body one by one at the same time with

* Corresponding author at: Department of Radiology, Fujian Cancer Hospital, Fujian Medical University Cancer Hospital, Fuzhou City, Fujiang Province 350014, China.
E-mail address: lutaocell@163.com (T. Lu).
Peer review under responsibility of King Saud University.

Production and hosting by Elsevier

https://doi.org/10.1016/j.sjbs.2020.02.016
1319-562X/

highly sensitive detectors such as X-ray beams, γ rays and ultrasounds that are precisely collimated (Evangelista et al., 2019). Due to its advantages such as fast scanning as well as high definition image, it has been widely used in the diagnosis of various diseases (Zhou et al., 2017). In terms of the human soft tissue, its difference of density is not big. In addition, the CT scan relies on its high-density resolution to form contrast and generate images (Fan et al., 2017). Therefore, organs that are composed of soft tissue like brain, lung, liver as well as pelvic organs, etc. can be well displayed by CT. In addition, CT can show the lesion image on a good anatomical image background (Kim et al., 2017). Timmeren et al. (2017) reported that CT can be used as a biomarker of prognostic imaging (Timmeren et al., 2017). Li et al. (2017) established a prognosis model to predict the recurrence rate of NSCLC by using 34 artificial scoring imaging features describing lesions, lung and chest, and 219 automatically extracted quantitative CT imaging radiology features describing lesions. The prognosis model can predict the progress of disease 3 months after stereotactic body radiotherapy. It enables doctors to make better clinical decisions (Li et al., 2017).

To sum up, the current studies on the prognosis model of NSCLC are mostly based on a single method to select characteristics, which has little reference value. To improve the accuracy as well as reliability of NSCLC prognosis model, by collecting CT scan data of NSCLC patients as the research object, a variety of feature selection methods were used to establish different prognosis models. Its reliability and performance were analyzed and compared, so as to discuss the application of radiomics of CT images in NSCLC on the basis of prognosis model, and to provide reference for the diagnosis of NSCLC in clinic.

2. Materials and methods

2.1. Patients

CT scan data of 200 NSCLC patients in our hospital (August 2013–December 2018) were collected, ranging from 28 to 78 years old. The average age is 60.74 years old. The height is 167.53 ± 10. 64 cm, and the weight is 61.31 ± 5.64 kg. The study was approved by the hospital ethics committee, and the patients signed relevant informed consent.

Inclusion criteria (Bianconi et al., 2018): all patients were confirmed to have NSCLC by surgery or biopsy. The clinical data of the patients were perfect. The contrast-enhanced CT image data were all standard CT images.

Exclusion criteria: patients with severe artifacts on CT images; patients with a large number of blood vessels passing through the lesion or close to the hilum of the lung that can't be accurately segmented; patients with incomplete clinical data.

2.2. Image segmentation

All CT images were acquired from the Philips Sence and Simplicity Brilliance iCT256 scanner. The image data was input into the workstation and processed with 3D-Slicer software to obtain the axial, sagittal as well as coronal 3D images of CT images. The lesions were analyzed, the tumor region and the non-tumor region were divided manually, and the grow-cut algorithm was used for interactive segmentation, so as to obtain more accurate tumor segmentation results. The analysis and processing work of image was jointly undertaken by two senior radiologists. If there was disagreement, it could consult the director of radiology for consultation and discussion.

2.3. Extraction of histological features of CT images

To eliminate the noise in the image and avoid unnecessary calculation, it quantified the segmented tumor through the histogram characteristics of high-dimensional image to obtain more accurate internal tumor conditions. The radiomics features (RF) of CT images included three-dimensional morphological features, grayscale features, texture features and wavelet features. The feature extraction (535 in total) was divided into four parts: first, the calculation of three-dimensional features (7), including tumor volume, surface area, compactness, spherical asymmetry, sphericity, as well as surface volume ratio; second, calculation of first-order statistical characteristics (14), including energy, entropy, kurtosis, mean, maximum, mean absolute deviation, median, minimum, span, root mean square, skewness, standard deviation, uniformity, variance; third, the calculation of texture features (52), including four categories of gray level symbiosis matrix, gray level run length matrix, gray level area matrix as well as neighborhood gray level difference matrix; fourth, the calculation of wavelet transform features (462). Feature Extraction toolbox software was used to complete all Feature Extraction. Thirty patients were randomly selected from the 200 enrolled patients for RF extraction. The lesions were re-analyzed by two senior radiologists, tumor areas and non-tumor areas were manually divided, and the RF of CT image were extracted. The intra-class correlation coefficient (ICC) was calculated to analyze the stability of the RF of CT images. If ICC was greater than 0.75, then the stability of the feature was good; if ICC was less than 0.75, then the stability of the feature was poor.

2.4. Selection of RF of CT images for lung cancer

100 patients were randomly selected from 200 enrolled patients, 11 classical feature selection methods were used to carry out variable selection experiments, and the RF of CT images with modeling ability were selected from 535 RF of CT images. 11 classic feature selection methods include Fisher's linear discriminant (FSCR), RELF, Minimum Redundancy Maximum Relevance (MRMR), Interaction Capping (ICAP), Gini Coefficient (GINI), Mutual Information Feature Selection (MIFS), Joint Mutual Information (JMI), Conditional Informax Feature Extraction (CIFE), Conditional Mutual Information Maximization (CMIM), Double Input Symmetric Relevance (DISR), and T-test Score (TSCR).

2.5. Establishment of prognostic model of images radiomics for NSCLC

Iterative learning of tumor features was performed by nine classifiers, including partial least squares (PLS), regularized discriminant analysis (RDA), random forest (RF), support vector machines (SVM), neural network (NNET), NB, generalized linear models (GLM), multi adaptive regression splines (MARS), as well as nearest neighbor (NN). Then, a prognostic model for the survival time of lung cancer patients was established. 100 patients selected from the selection of the RF of CT images of lung cancer, including the group with a longer survival time (58 cases) and the group with a shorter survival time (42 cases), were selected. The distribution of various characteristics was standardized, and the survival curve of subjects was drawn to evaluate the performance of the prognostic model obtained.

2.6. Cross-validation of prognostic model of images radiomics

The performance of the prognostic model of the nine classifiers was tested by K-fold cross-validation test. Among the 200 patients enrolled, 100 patients were excluded from the selection of the RF of CT images of lung cancer, and the remaining 100 patients were

selected for performance evaluation of model. The data of 100 patients were randomly divided into 5 sets for 5-fold cross-validation. One set was selected as the test set each time, and the rest set was the training set. Each classifier and feature extraction algorithm were combined respectively. It was necessary to repeat five-fold cross-validation five times to calculate the reliability of the classification model.

2.7. Selection of the number of optimal features

The relationship between the classification performance of the nine classifiers and the number of features in the selection of the RF of CT images of lung cancer was analyzed. According to the representation ability of each feature in different feature selection methods, the contribution degree of each feature in the combination of each feature selection algorithm and classifier was sorted. According to the information representation ability of various features, a total of 7 groups of features (i.e., 35 features) were trained on 99 classification models at an interval of 5, and then the reliability of each prognostic model was verified by 5-fold cross validation. In addition, combined with the optimal features obtained by 11 feature selection algorithms, a prediction model based on global optimal features was established for each classifier. Each classification model was trained with 5, 10, 15, 20, 25, 30, and 35 features to analyze the relationship between the reliability of each model and the number of features.

2.8. Performance evaluation of prognostic models

According to the training and reliability of the prognostic model, the prognostic model with the highest reliability in each algorithm combination was applied to the test set data. The performance of the model with global optimal features is evaluated by classification accuracy as well as area under the subject characteristic curve (AUC) indexes. The performance of the prognostic model with 11 feature selection algorithms and single feature selection algorithm was analyzed and compared. The test set was selected to detect the prognosis model, and the receiver operating characteristic curve was drawn according to the positive rates of true as well as false.

2.9. Statistical method

Excel was used to establish the database, and SPSS22.0 statistical software was used for statistical analysis. Quantitative data that conformed to the normal distribution were expressed by mean ± standard deviation. T-test was used for comparison between groups. For quantitative data that did not conform to normal distribution, rank-sum test was used for comparison among groups, and chi-square test was used for comparison among different groups. $P < 0.05$ indicated statistically significant.

3. Results and discussion

3.1. Evaluation results of the stability of RF extraction of CT images

The results of the stability evaluation of the RF of CT image of patients with NSCLC were shown in Fig. 1. It can be concluded that the intra-group correlation coefficient with 6 features was lower than 0.75 and had poor stability, accounting for 1.12% (6 / 535) of the original features. And the intra-group correlation coefficients of other features were all higher than 0.75, with good stability, accounting for 98.88% (529 / 535) of the original features.

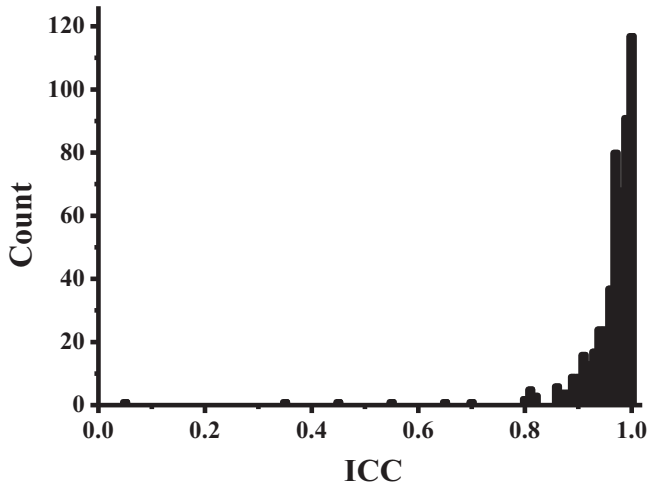

Fig. 1. Evaluation of the stability of the RF of CT images of patients with NSCLC.

3.2. Reliability evaluation of prognostic model based on optimal features of specific algorithms

The prognostic models of NSCLC with the combination of 11 feature selection algorithms and 9 classifiers were trained with different feature numbers, and the 20 combinations with the highest reliability of the prognostic models were selected, as shown in Table 1. From the combination of these 20 prognostic models, it can be concluded that five prognostic models have the highest reliability when the five optimal features are used for training. When 10 optimal features were used for training, 4 prognostic models combinations achieved the highest reliability. When 15 optimal features were used for training, no combination of prognostic models had the highest reliability. When 20 optimal features were used for training, 6 combinations of prognostic models had the highest reliability. When 25 optimal features were used for training, 1 prognostic model combination had the highest reliability. When 30 optimal features were used for training, 1 prognostic model combination had the highest reliability. When 35 optimal features were used for training, the reliability of 3 prognostic models combinations reached the highest, suggesting that the number of features was an important factor affecting the reliability of prognostic models. Among these 20 combinations of prognostic models with the highest reliability, 8 combinations used RELF feature selection algorithm, 6 combinations used GIGI feature

Table 1
The 20 combinations with the highest reliability of the prognostic model.

Number of features	Feature selection algorithm	Classifier	Reliability
5	MIFS	SVM	0.8169
20	RELF	SVM	0.8114
10	RELF	RDA	0.7968
10	RELF	NNET	0.7937
35	JMI	RF	0.7905
20	RELF	PLS	0.7895
10	RELF	NN	0.7888
25	RELF	RF	0.7806
35	GINI	RF	0.7783
5	GINI	NNET	0.7734
5	GINI	SVM	0.7695
20	FSCR	RF	0.7673
5	GINI	NN	0.7638
20	GINI	NB	0.7635
30	RELF	NB	0.7598
20	TSCR	NB	0.7593
20	TSCR	NNET	0.7538
10	RELF	GLM	0.7526
35	TSCR	RF	0.7500
5	GINI	PLS	0.7455

Table 2
Reliability results of prognostic models based on global optimal features.

Number of features	PLS	RDA	RF	SVM	NNET	NB	GLM	MARS	NN
5	0.6548	0.6591	0.6699	0.6062	0.6579	0.5608	0.6538	0.6116	0.6081
10	0.7195	0.6813	0.7369	0.6692	0.6815	0.6585	0.7066	0.7352	0.6154
15	0.6925	0.6871	0.7398	0.7117	0.6387	0.6990	0.6982	0.7295	0.6897
20	0.6847	0.6524	0.7285	0.6713	0.6425	0.6999	0.6507	0.7130	0.6686
25	0.7315	0.6968	0.7339	0.7284	0.6336	0.7024	0.6658	0.7176	0.7283
30	0.7256	0.6832	0.7489	0.7308	0.6691	0.6821	0.6237	0.6882	0.6273
35	0.7103	0.6255	0.7416	0.7165	0.6460	0.6834	0.6001	0.7073	0.6835

selection algorithm, and 3 combinations used TSCR algorithm, suggesting that RELF, GINI, and TSCR feature selection algorithms had better feature selection performance. In addition, 5 combinations adopted RF classifier, 3 combinations adopted SVM classifier, 3 combinations adopted NNET classifier and 3 combinations adopted NB classifier, indicating that RF, SVM, NNET and NB classifier had better classification performance (see Table 2).

3.3. Reliability evaluation of prognostic model based on global optimal features

The different feature selection methods in the RF of CT images were statistically analyzed. According to the total number of times it was selected, the sequence of global optimal features was obtained, and the reliability of the prognostic model was quantitatively evaluated in accordance with this sequence, so as to explore whether feature selection has reference value for the established prognostic model. The prognostic model of NSCLC was established based on the global optimal characteristics, and the reliability results were shown in Table 1 and Fig. 2. When 25 global optimal features were adopted for training, the reliability of prognostic model of 4 classifiers reached the maximum. When 10 global optimal features were adopted for training, the reliability of prognostic model of 3 classifiers reached the maximum. The average reliability of these 9 classifiers after training based on the number of optimal features was 0.7180.

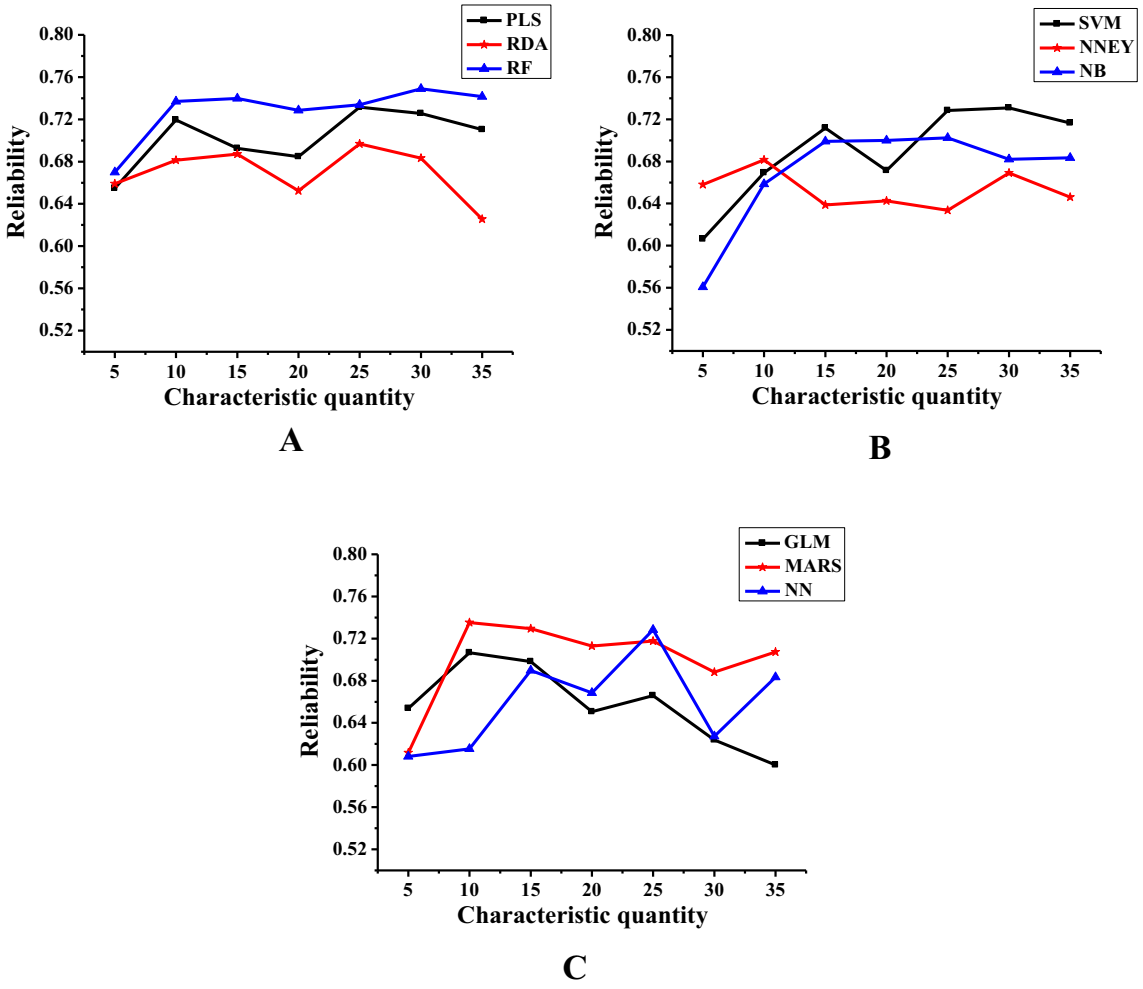

Fig. 2. Reliability results of prognostic models based on global optimal features (A is PLS, RDA and RF classifier, B is the SVM, NNET and NB classifiers, and C is the GLM, MARS and NN classifiers).

3.4. Evaluation of the performance of prognostic models based on the optimal number of feature of particular algorithm

Based on the optimal number of characteristics, the classification accuracy and the AUC of the 20 prognostic model combinations with the highest reliability selected were calculated to evaluate their performance. The results were shown in Table 3 and Fig. 3A, and the accuracy of the prognostic model was significantly correlated with the AUC. According to the reliability, accuracy and AUC results of each prognostic model, the best prognostic model with the best performance was: 30-RELF-NB, i.e. 30 optimal features, RELF feature selection algorithm and NB classifier. According to this combination, the 100 patients were divided into the groups with longer as well as shorter predicted survival time, and the subject survival curve was drawn, as shown in Fig. 3B. It can be concluded that there was a great difference between the group with a long predicted survival time and the group with a short predicted survival time.

Table 3
Evaluation of the performance of a prognostic model based on the optimal number of features of a specific algorithm.

No.	Number of features	Feature selection algorithm	Classifier	Accuracy rate	AUC
1	5	MIFS	SVM	0.6514	0.7140
2	20	RELF	SVM	0.7620	0.7542
3	10	RELF	RDA	0.7671	0.7995
4	10	RELF	NNET	0.7191	0.7710
5	35	JMI	RF	0.7884	0.8230
6	20	RELF	PLS	0.7404	0.7912
7	10	RELF	NN	0.7644	0.7538
8	25	RELF	RF	0.7901	0.7633
9	35	GINI	RF	0.7645	0.8315
10	5	GINI	NNET	0.7891	0.8075
11	5	GINI	SVM	0.7450	0.7690
12	20	FSCR	RF	0.7584	0.8210
13	5	GINI	NN	0.7193	0.7975
14	20	GINI	NB	0.7417	0.8205
15	30	RELF	NB	0.8155	0.8093
16	20	TSCR	NB	0.7904	0.8663
17	20	TSCR	NNET	0.8133	0.7882
18	10	RELF	GLM	0.7424	0.7792
19	35	TSCR	RF	0.7821	0.8340
20	5	GINI	PLS	0.7676	0.8022

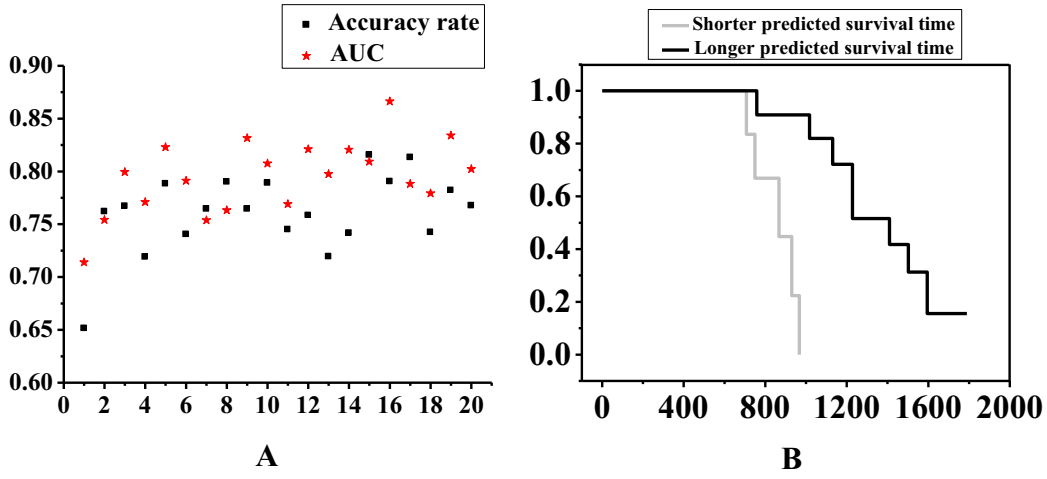

Fig. 3. A prognostic model based on the optimal number of features of a specific algorithm (A: performance evaluation results; B: survival curve of subjects).

Table 4
Evaluation results of the performance of prognostic models based on the number of global optimal features.

No.	Number of features	Classifier	Accuracy rate	AUC
1	25	PLS	0.7856	0.9015
2	25	RDA	0.8127	0.8912
3	30	RF	0.8413	0.8693
4	30	SVM	0.7400	0.6275
5	10	NNET	0.7598	0.8637
6	25	NB	0.8875	0.9365
7	10	GLM	0.7429	0. 8412
8	10	MARS	0.7901	0.8056
9	25	NN	0.6225	0.6573

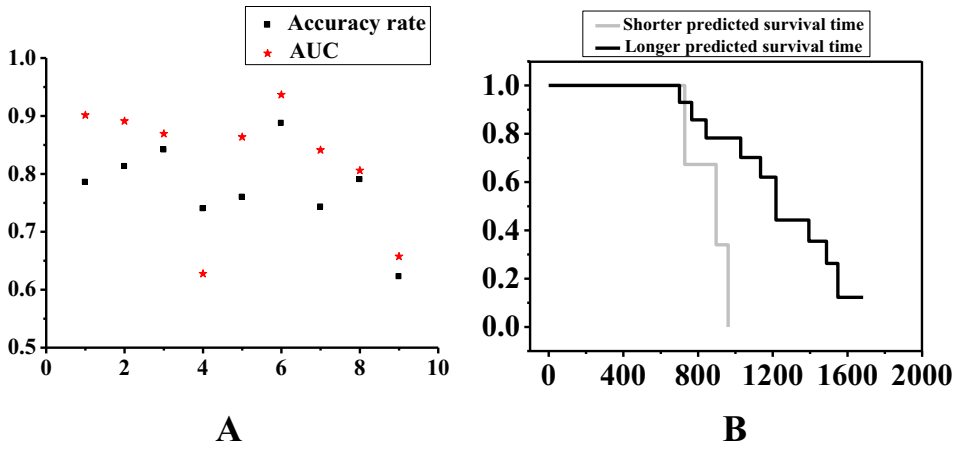

Fig. 4. A prognostic model based on the number of global optimal features (A: performance evaluation results; B: survival curve of subjects).

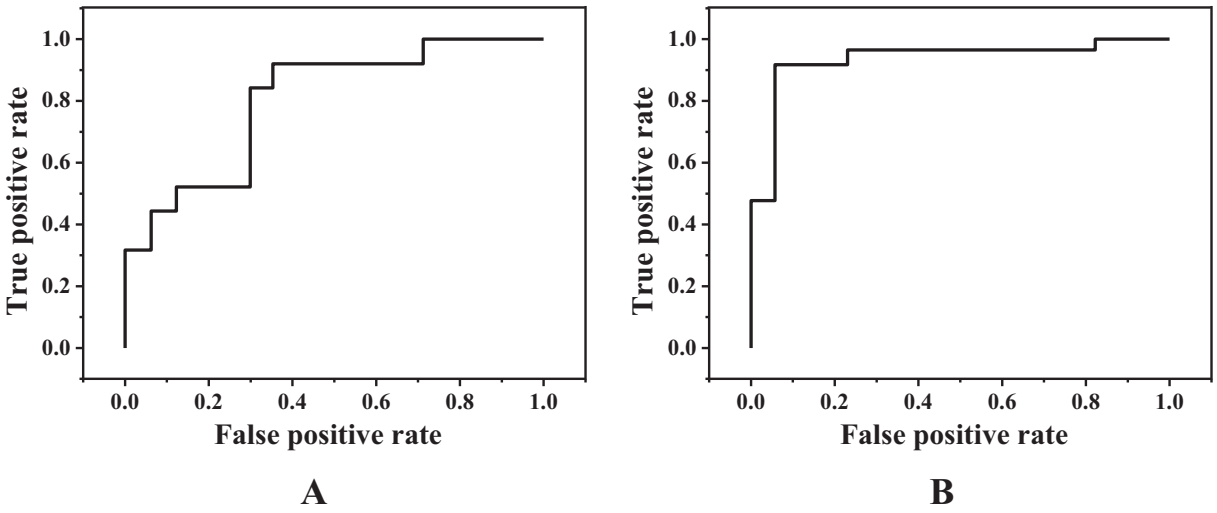

Fig. 5. The characteristic curves of subjects with a combination of two feature selection protocol prognostic models (A: combination of 30-RELF-NB prognostic models based on the optimal number of features of a specific algorithm; B: combination of 25-NB prognostic models based on the number of global optimal features).

3.5. Performance evaluation of prognostic model based on global optimal feature number

Based on the number of global optimal features, the classification accuracy and AUC of the established prognostic model of NSCLC were calculated. The results were shown in Table 4 as well as Fig. 4A. It can be concluded that among all models, NB prognostic model (feature number: 25) had the highest accuracy and AUC. The subject survival curve was shown in Fig. 4B, which showed that there was a great difference between the group with a long predicted survival time and the group with a short predicted survival time.

3.6. Comparison of performance of prognostic models with two feature selection schemes

The performances of the prognostic model of the two feature selection schemes were compared, and the subject characteristic curve was shown in Fig. 5. 30-RELF-NB was the best combination of prognosis models based on the optimal number of features of specific algorithm, with an accuracy of 0.8155 and AUC of 0.8093. The optimal combination of prognostic models based on the number of global optimal features was 25-NB, with an accuracy of 0.8875 and AUC of 0.9365. The results showed the accuracy and AUC of the prognostic model based on the global optimal features were higher than those based on the features constructed by the single feature selection algorithm. Therefore, the reliability of the prognosis model could be improved by using the prognosis model based on the global optimal characteristics to classify the cases.

4. Conclusion

Through the application of radiomics of CT images in NSCLC based on the prognostic model, it was found that the number of features used in the prognostic model had great influence on the reliability of the model. For different models, the number of features that made their reliability reach the highest was also different. In addition, the prognostic model based on global optimal features had higher overall stability than the one based on feature training of specific feature selection algorithm. However, there are some deficiencies in the study. For example, the size of the sample is small, which results in a certain degree of deviation. Therefore, in the later research process, it is necessary to increase the data capacity to make the obtained results more valuable for reference.

References

Namkoong, M., Moon, Y., Park, J.K., 2017. Lobectomy versus sublobar resection in non-lepidic small-sized non-small cell lung cancer[J]. Korean J. Thor. Cardiovasc. Surg. 50 (6), 415–423.

Huang, Y., Soo, R.A., 2017. The KEY to the end of chemotherapy in non-small cell lung cancer?[J]. Ann. Transl. Med. 5 (7), 166.

Casiraghi, M., Eng, P.M., Piperno, G., et al., 2017. Salvage surgery after definitive chemo-radiotherapy for non-small cell lung cancer[J]. Semin. Thorac. Cardiovasc. Surg. 29 (2), 233–241.

Beth Eaby-Sandy, M.C.O., 2017. Use of diagnostic tests in advanced non-small cell lung cancer[J]. J. Adv. Practition. Oncol. 8 (2), 173–185.

Kato, Y., Kashima, J., Watanabe, K., et al., 2018. Association between clinicopathological features and programmed death ligand 1 expression in non-small cell lung cancer[J]. Antican. Res. 38 (2), 1077–1083.

Namani, A., Cui, Q.Q., Wu, Y., et al., 2017. NRF2-regulated metabolic gene signature as a prognostic biomarker in non-small cell lung cancer[J]. Oncotarget, 2017;8 (41):69847–69862 (Liang J, Li Z, Zhang Y, et al. [Analysis of factors affecting the prognosis of ICU patients by multiple logistic regression model: a retrospective cohort study of 1 299 patients in 12 consecutive years][J]. Zhonghua Wei Zhong Bing Ji Jiu Yi Xue, 2017, 29(7):602).

Hui, R., Garon, E.B., Goldman, J.W., et al., 2017. Pembrolizumab as first-line therapy for patients with PD-L1-positive advanced non-small cell lung cancer: a phase 1 trial.[J]. Ann Oncol Off J Eur Soc Med. Oncol. 28 (4), 874–881.

Lin, G.N., Peng, J.W., Liu, P.P., et al. Elevated neutrophil-to-lymphocyte ratio predicts poor outcome in patients with advanced non-small-cell lung cancer receiving first-line gefitinib or erlotinib treatment[J]. Asia-Pacific J. Clin. Oncol., 2017, 13 (5):2696–703.

Kamaleshwaran, K.K., Joseph, J., Kalarikal, R.K., et al. Image findings of rare case of peritoneal carcinomatosis from non small cell lung cancer and response to Erlotinib in F-18 FDG positron emission tomography/computed tomography:[J]. Ind. J. Nucl. Med. Ijnm Off. J. Soc. Nucl. Med. India, 2017;32(2):140–142.

Evangelista, L., Cuppari, L., Menis, J., et al., 2019. 18F-FDG PET/CT in non-small-cell lung cancer patients: a potential predictive biomarker of response to immunotherapy[J]. Nucl. Med. Commun. 40 (8), 1.

Zhou, Y., Gao, S., Huang, Y., et al., 2017. A pilot study of18F-alfatide PET/CT imaging for detecting lymph node metastases in patients with non-small cell lung cancer:[J]. Sci. Rep. 7 (1), 2877.

Fan, J.L., Zhai, K.K., Ren, T.T., et al., 2017. Distant Metastasis and survival outcomes after computed tomography-guided needle biopsy in Stage I-II non-small cell lung cancer[J]. Zhongguo fei ai za zhi = Chinese J. Lung Can. 20 (3), 187–191.

Kim, H., Yoo, I.R., Boo, S.H., et al., 2017. Prognostic value of pre- and post-treatment FDG PET/CT parameters in small cell lung cancer patients[J]. Nucl Med Mol Imaging 52 (1), 31–38.

Timmeren, J.E.V., Leijenaar, R.T.H., Elmpt, W.V., et al., 2017. Survival prediction of non-small cell lung cancer patients using radiomics analyses of cone-beam CT images[J]. Radiother. Oncol. 123 (3), 363.

Li, Q., Kim, J., Balagurunathan, Y., et al., 2017. CT imaging features associated with recurrence in non-small cell lung cancer patients after stereotactic body radiotherapy[J]. Radiat. Oncol. 12 (1), 158.

Bianconi, F., Fravolini, M.L., Bello-Cerezo, R., et al., 2018. Evaluation of shape and textural features from CT as prognostic biomarkers in non-small cell lung cancer[J]. Antican. Res. 38 (4), 2155–2160.